First Direct Measurement of the $^2H(\alpha,\gamma)^6Li$ Cross Section at Big Bang Energies and the Primordial Lithium Problem

M. Anders,[1,2,†] D. Trezzi,[3] R. Menegazzo,[4] M. Aliotta,[5] A. Bellini,[6] D. Bemmerer,[1] C. Broggini,[4] A. Caciolli,[4] P. Corvisiero,[6] H. Costantini,[6,‡] T. Davinson,[5] Z. Elekes,[1] M. Erhard,[4,§] A. Formicola,[7] Zs. Fülöp,[8] G. Gervino,[9] A. Guglielmetti,[3] C. Gustavino,[10,‖] Gy. Gyürky,[8] M. Junker,[7] A. Lemut,[6,*] M. Marta,[1,¶] C. Mazzocchi,[3,**] P. Prati,[6] C. Rossi Alvarez,[4] D. A. Scott,[5] E. Somorjai,[8] O. Straniero,[11,12] and T. Szücs[8]
(LUNA Collaboration)

[1]*Helmholtz-Zentrum Dresden-Rossendorf, Bautzner Landstrasse 400, 01328 Dresden, Germany*
[2]*Technische Universität Dresden, Mommsenstrasse 9, 01069 Dresden, Germany*
[3]*Università degli Studi di Milano and INFN, Sezione di Milano, Via G. Celoria 16, 20133 Milano, Italy*
[4]*INFN, Sezione di Padova, Via F. Marzolo 8, 35131 Padova, Italy*
[5]*SUPA, School of Physics and Astronomy, University of Edinburgh, EH9 3JZ Edinburgh, United Kingdom*
[6]*Università degli Studi di Genova and INFN, Sezione di Genova, Via Dodecaneso 33, 16146 Genova, Italy*
[7]*Laboratori Nazionali del Gran Sasso (LNGS), Via G. Acitelli 22, 67100 Assergi, Italy*
[8]*Institute of Nuclear Research (MTA ATOMKI), PO Box 51, HU-4001 Debrecen, Hungary*
[9]*Università degli Studi di Torino and INFN, Sezione di Torino, Via P. Giuria 1, 10125 Torino, Italy*
[10]*INFN, Sezione di Roma "La Sapienza", Piazzale A. Moro 2, 00185 Roma, Italy*
[11]*Osservatorio Astronomico di Collurania, Via M. Maggini, 64100 Teramo, Italy*
[12]*INFN, Sezione di Napoli, Via Cintia, 80126 Napoli, Italy*

(Received 21 January 2014; revised manuscript received 8 April 2014; published 21 July 2014)

Recent observations of ^{6}Li in metal poor stars suggest a large production of this isotope during big bang nucleosynthesis (BBN). In standard BBN calculations, the $^2H(\alpha,\gamma)^6Li$ reaction dominates ^{6}Li production. This reaction has never been measured inside the BBN energy region because its cross section drops exponentially at low energy and because the electric dipole transition is strongly suppressed for the isoscalar particles ^{2}H and α at energies below the Coulomb barrier. Indirect measurements using the Coulomb dissociation of ^{6}Li only give upper limits owing to the dominance of nuclear breakup processes. Here, we report on the results of the first measurement of the $^2H(\alpha,\gamma)^6Li$ cross section at big bang energies. The experiment was performed deep underground at the LUNA 400 kV accelerator in Gran Sasso, Italy. The primordial $^6Li/^7Li$ isotopic abundance ratio has been determined to be $(1.5 \pm 0.3) \times 10^{-5}$, from our experimental data and standard BBN theory. The much higher $^6Li/^7Li$ values reported for halo stars will likely require a nonstandard physics explanation, as discussed in the literature.

DOI: 10.1103/PhysRevLett.113.042501 PACS numbers: 25.55.−e, 25.40.Lw, 26.35.+c, 98.80.Ft

In its formulation, the standard big bang nucleosynthesis (in the following, standard big bang nucleosynthesis will be referred just as BBN) occurs during the first minutes of the Universe, with the formation of light isotopes such as ^{2}H, ^{3}He, ^{4}He, ^{6}Li, and ^{7}Li. Their abundances only depend on standard model physics, on the baryon-to-photon ratio and on the nuclear cross sections of involved processes. The observed ^{2}H and ^{4}He abundances are in good agreement with calculations, confirming the overall validity of BBN theory [1]. By contrast, the amount of ^{7}Li predicted by BBN is higher than that observed in primitive, metal-poor halo stars ("the lithium problem") [2]. This puzzling discrepancy was further exacerbated by a recent high-precision determination of the baryon-to-photon ratio (see Refs. [3,4] and references therein): BBN ^{7}Li predictions are now a factor 2–4 higher than observations [1].

A nuclear physics solution to the ^{7}Li problem is highly improbable, because of accurate measurements at BBN energies, obtained, e.g., at the Laboratory for Underground Nuclear Astrophysics (LUNA) facility deep underground [5,6].

Conversely, the amount of ^{6}Li predicted by the BBN is about 3 orders of magnitude lower than the observed one in metal-poor stars ("the second lithium problem"). Asplund *et al.* surveyed a number of metal-poor stars for ^{6}Li and reported values of $^6Li/^7Li \sim 5 \times 10^{-2}$ in about a dozen cases [7,8]. Recently, many of the claimed ^{6}Li detections have been debated [9] but for a few metal-poor stars a significant excess of ^{6}Li has been confirmed [1,10]. In contrast, BBN results provide $^6Li/^7Li = 2^{+3}_{-2} \times 10^{-5}$ [11], much below the detected levels. The difference between observed and calculated $^6Li/^7Li$ ratios may reflect unknown postprimordial processes or physics beyond the standard model [1]. However, before nonstandard scenarios can be invoked, it is necessary to better constrain the nuclear physics inputs.

BBN production of ^{6}Li is dominated by just one nuclear reaction, $^2\mathrm{H}(\alpha,\gamma)^6\mathrm{Li}$. At low energies, this reaction has been studied previously: by detection of the ^{6}Li residual nucleus [12], by in-beam γ spectroscopy at the $E = 0.711$ MeV resonance [13], and in two separate Coulomb dissociation experiments at 26 and 150 MeV/A ^{6}Li projectile energy, respectively [14,15]. (In this context, E refers to the center-of-mass energy and E_α to the $^4\mathrm{He}^+$ projectile energy in the laboratory system.) However, Ref. [15] reported detecting such a high background from nuclear breakup that no cross section could be extracted, a problem that should get worse at lower projectile energy. Moreover, since $E2$ transitions dominate the Coulomb dissociation, the 26 MeV/A cross section data [14] may be interpreted as upper limits of the $E2$ component. Reference [15] also reported a theoretical excitation function that was to some extent corroborated by the reconstructed angular distribution of the excited ^{6}Li nuclei. Finally, an attempt to measure the $^2\mathrm{H}(\alpha,\gamma)^6\mathrm{Li}$ cross section at BBN energies resulted in an upper limit [16].

The $^2\mathrm{H}(\alpha,\gamma)^6\mathrm{Li}$ cross section $\sigma_{24}(E)$ can be parameterized by the astrophysical S factor $S_{24}(E)$ given by

$$S_{24}(E) = \sigma_{24}(E) E \exp\left[72.44/\sqrt{E(\mathrm{keV})}\right]. \quad (1)$$

To precisely determine BBN ^{6}Li production, $\sigma_{24}(E)$ has to be measured directly at astrophysically relevant energies $[30 \lesssim E(\mathrm{keV}) \lesssim 400]$. Because of the low expected counting rate, such an experiment requires a deep underground accelerator laboratory such as LUNA, where the background in a shielded γ-ray detector reaches unmatched low levels [17]. LUNA is operated in the Gran Sasso National Laboratory (LNGS), Italy, shielded from cosmic rays by 1400 m of rock. Several nuclear reactions of astrophysical importance have been studied at very low energies at LUNA in recent years [18,19].

In this Letter, new LUNA cross section data on the $^2\mathrm{H}(\alpha,\gamma)^6\mathrm{Li}$ reaction at BBN relevant energies are presented. At low energies, the $^2\mathrm{H}(\alpha,\gamma)^6\mathrm{Li}$ reaction proceeds either via electric dipole ($E1$) or electric quadrupole ($E2$) direct capture to the ground state of ^{6}Li, in either case emitting a single γ ray.

The measurement is based on the use of the 400 kV accelerator [20] that provides an α beam of high intensity. Figure 1 shows the experimental setup (see Ref. [21] for details). Briefly, it consists of a windowless gas target filled with 0.3 mbar deuterium gas and a large (137% relative efficiency) high-purity germanium (HPGe) detector placed at a 90° angle with respect to the ion beam direction, in very close geometry. The $^4\mathrm{He}^+$ beam (typical intensity 0.3 mA) passes a series of long, narrow apertures before entering the target chamber and is stopped on a copper beam dump that forms part of a beam calorimeter with constant temperature gradient. The natural background of LNGS is further reduced by means of a 4π lead shield around the reaction chamber and the HPGe detector. The setup is enclosed in an

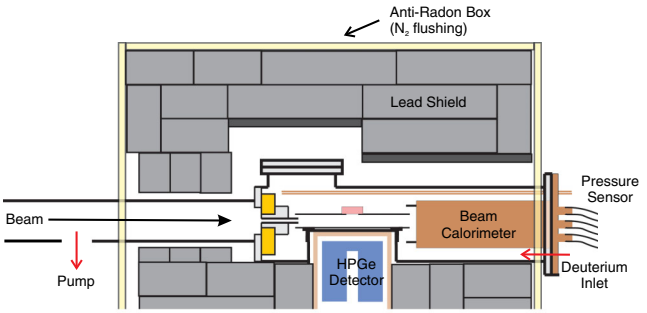

FIG. 1 (color online). Sketch of experimental setup. See text for a general description and Ref. [21] for further details.

antiradon box flushed with high purity N_2, to reduce and stabilize the γ activity from the radon decay chain. The main source of remaining background is of beam-induced nature and is due to energetic deuterons from elastic scattering of the $^4\mathrm{He}^+$ beam on the deuterium. These deuterons produce neutrons via the $^2\mathrm{H}(d,n)^3\mathrm{He}$ reaction ($Q = 3.267$ MeV). Subsequent inelastic neutron scattering reactions in the structural and shielding materials and (mainly) in the germanium detector give rise to a large Compton background in the $^2\mathrm{H}(\alpha,\gamma)^6\mathrm{Li}$ region of interest (ROI). A detailed study of the neutron induced background, and the experimental steps taken to reduce it, has already been reported [21]. Its value is one order of magnitude lower than room (or natural) background at Earth's surface [22], but remains a factor of 10 higher than the expected signal. Since the shape and rate of the beam-induced background depend only weakly on the $^4\mathrm{He}^+$ beam energy [21], an irradiation at one given beam energy can be used as a background monitor for an irradiation at a different beam energy, provided that the two γ-ray ROIs do not overlap. For the adopted energies of $E_\alpha = 280$ and 400 keV, the no-overlap criterion is fulfilled.

As discussed above, the HPGe spectral rate $R(E_\gamma)_i$ at a given beam energy $E_{\alpha,i}$ is composed by the neutron induced background $\mathrm{BG}_{\mathrm{neutron}}(E_\gamma)_i$, the natural background $\mathrm{BG}_{\mathrm{room}}(E_\gamma)$, and the γ-ray contribution $N(E_\gamma)_i$ from the $^2\mathrm{H}(\alpha,\gamma)^6\mathrm{Li}$ reaction. Therefore, the $\mathrm{BG}_{\mathrm{neutron}}(E_\gamma)_i$ rate can be written as follows:

$$\mathrm{BG}_{\mathrm{neutron}}(E_\gamma)_i = R(E_\gamma)_i - \mathrm{BG}_{\mathrm{room}}(E_\gamma) - k_i N(E_\gamma)_i, \quad (2)$$

where the parameter k_i is proportional to the $^2\mathrm{H}(\alpha,\gamma)^6\mathrm{Li}$ reaction cross section. Assuming that the rate of neutron induced background $\mathrm{BG}_{\mathrm{neutron}}(E_\gamma)_{280}$ has the same structure as the $\mathrm{BG}_{\mathrm{neutron}}(E_\gamma)_{400}$, we have

$$\mathrm{BG}_{\mathrm{neutron}}(E_\gamma)_{400} = \beta \mathrm{BG}_{\mathrm{neutron}}(E_\gamma)_{280}. \quad (3)$$

More rigorously, the structure of the neutron induced background weakly depends on the beam energy [21]. Consequently, the β parameter weakly depends on E_γ[21],

as it will be discussed in the following. Two analysis procedures have been developed. Method A is based on selecting flat, Compton-dominated regions in the observed γ-ray spectra [21,23]. Method B determines the free parameters β and k_i by a MINUIT χ^2 (least squares) minimization routine that uses the full statistics in the 1500–1625 keV γ-ray energy region. The results from both methods are mutually consistent; method B is used henceforth.

The relationship used in the minimization procedure is obtained by combining Eq. (3) with Eq. (2). As already remarked, the $\mathrm{BG}_{\mathrm{neutron}}(E_\gamma)_i$ spectral shape weakly depends on the beam energy: the gap between the two energies considered for the α beam (120 keV) is relatively small with respect to the energy of neutrons produced in the $^2\mathrm{H}(d,n)^3\mathrm{He}$ reaction ($E_n = 2450$ keV in the center-of-mass system). The $\mathrm{BG}_{\mathrm{neutron}}(E_\gamma)_{280}$ and the $\mathrm{BG}_{\mathrm{neutron}}(E_\gamma)_{400}$ spectra have been extensively studied by means of a dedicated simulation [21]. One difference between the simulated spectra at the two beam energies, also observed in the data, is the strength of the γ line at $E_\gamma = 1811$ keV due to the deexcitation of ^{56}Fe nuclei, somewhat more intense in the $\mathrm{BG}_{\mathrm{neutron}}(E_\gamma)_{400}$ spectrum. The Compton edge for this particular γ ray lies exactly between the ROI_{400} and the ROI_{280}. Therefore, the 1811 keV γ-ray contribution to the $\mathrm{BG}_{\mathrm{neutron}}(E_\gamma)_i$ spectra has been subtracted. The other effect predicted by the simulation and experimentally observed is the overall gamma energy dependence of the ratio of the two spectra. This effect has been considered by correcting the shape of the $\mathrm{BG}_{\mathrm{neutron}}(E_\gamma)_{280}$ spectrum using a polynomial fit in the energy window of minimization.

The in-beam measurements at the two beam energies have been alternated during the ~40 days of acquisition time (about 20 days for each beam energy). The total data sample is divided into two subsamples (run 1 and run 2), acquired in two different periods due to the accelerator availability for this measurement. The collected charge is approximately the same at each energy, i.e., about 550 C. As expected, the relevant parts of the γ-ray spectrum for the two runs (Fig. 2) show an excess in the 400 keV ROI.

The yields at $E_\alpha = 400$ keV and $E_\alpha = 280$ keV give astrophysical S factors ($\chi^2/N_{\mathrm{DOF}} = 0.76$, where N_{DOF} is the number of degrees of freedom),

$$S_{24}(134\,\mathrm{keV}) = (4.0^{+0.8\,(\mathrm{stat})}_{-0.9} \pm 0.5^{(\mathrm{syst})}) \times 10^{-6}\,\mathrm{keV}\,b, \quad (4)$$

$$S_{24}(94\ \mathrm{keV}) = (2.7^{+1.5\,(\mathrm{stat})}_{-1.6} \pm 0.3^{(\mathrm{syst})}) \times 10^{-6}\ \mathrm{keV}\,b. \quad (5)$$

The minimization has been performed considering the counting excesses inside the ROIs without any *a priori* assumption on the gamma-ray angular distribution. The statistical error is obtained in the minimization procedure, where the correlation between β, k_{400}, and k_{280} is computed by means of the covariance matrix. The total systematic uncertainty (target density, beam heating, beam intensity, gamma detection efficiency) amounts to 13% [23]. The

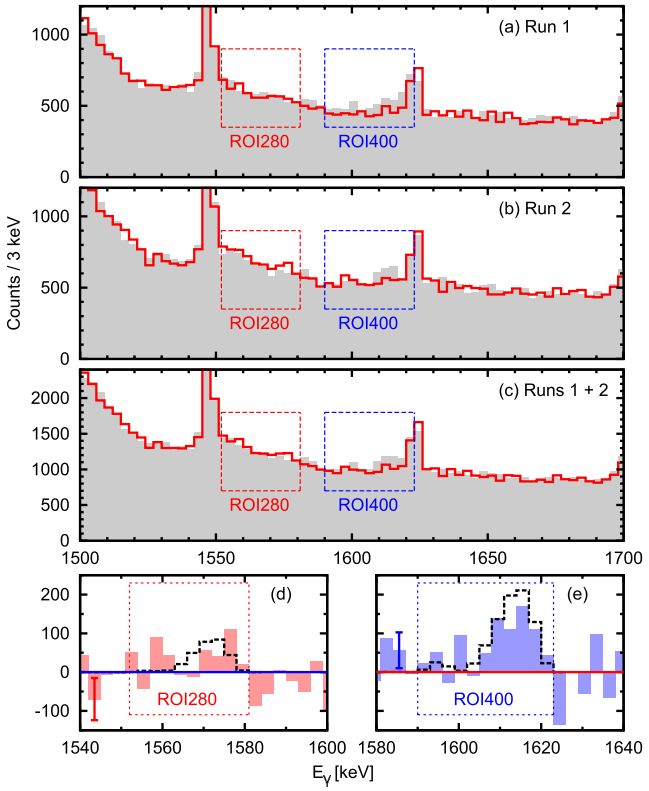

FIG. 2 (color online). (a), (b), and (c) show relevant parts of the γ-ray spectrum for runs 1, 2, and their sum, after subtraction of natural background. The $E_\alpha = 400$ keV data are shown as filled gray histograms, the rescaled (see text) 280 keV data as empty red histograms. (d) and (e) show the $E_\alpha = 280$ and 400 keV spectrum, respectively, as filled histogram, after background subtraction as described in the text. One representative error bar is shown. The dashed line represents the expected γ-ray line shape based on the Mukhamedzhanov theoretical description of the angular distribution for the $^2\mathrm{H}(\alpha,\gamma)^6\mathrm{Li}$ reaction [24].

1811 keV gamma-ray contribution subtracted from the $\mathrm{BG}_{\mathrm{neutron}}(E_\gamma)_i$ spectra has been found to be negligible: it corrects the $S_{24}(134\ \mathrm{keV})$ value for less than 1% and the $S_{24}(94\ \mathrm{keV})$ for less than 3%. Likewise, the effect of the correction with the polynomial fit (see above) is about 5% on $S_{24}(134\ \mathrm{keV})$ and 14% on $S_{24}(94\ \mathrm{keV})$.

The counting excess at $E_\alpha = 400$ keV has a significance exceeding 4 standard deviations while the counting excess at $E_\alpha = 280$ keV has a lower significance as a consequence of the higher Coulomb barrier and of the absence of resonant nuclear effects. The shape of the counting excess suggests a forward-backward asymmetry of emitted photons, possibly due to the interference between dipole and quadrupole transitions. The level and the shape of the counting excess obtained at $E_\alpha = 400$ keV are in good agreement with the yield and the angular distribution for the $^2\mathrm{H}(\alpha,\gamma)^6\mathrm{Li}$ reaction computed by Mukhamedzhanov [24]. The analysis has therefore been repeated by generating $N(E_\gamma)_i$ according to the Mukhamedzhanov angular distribution. The setup geometry, the calibration of the

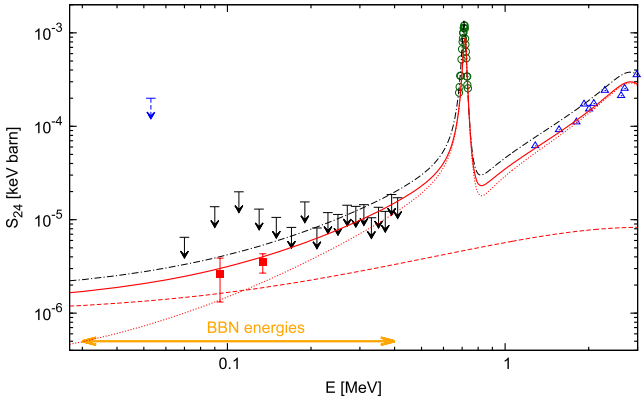

FIG. 3 (color online). Astrophysical S factor of the $^2\mathrm{H}(\alpha,\gamma)^6\mathrm{Li}$ reaction from the present Letter (red squares) and from the literature (data: blue triangles [12], green circles [13]; upper limits: black arrows [14], blue dashed arrow [16]; theory: red long dashed = $E1$ [24], red short dashed = $E2$ [24], red full = $E1 + E2$ [24], black dot dashed = $E1 + E2$ [15]).

germanium detector, and the Doppler effect have been considered. The S factors obtained in this way are ($\chi^2/N_{\mathrm{DOF}} = 0.84$)

$$S_{24}(134\ \mathrm{keV}) = (3.5^{+0.6}_{-0.7}{}^{(\mathrm{stat})} \pm 0.5^{(\mathrm{syst})} \pm 0.5^{(\mathrm{model})}) \times 10^{-6}\ \mathrm{keV}\,b, \quad (6)$$

$$S_{24}(94\ \mathrm{keV}) = (2.6^{+1.2}_{-1.3}{}^{(\mathrm{stat})} \pm 0.3^{(\mathrm{syst})} \pm 0.5^{(\mathrm{model})}) \times 10^{-6}\ \mathrm{keV}\,b, \quad (7)$$

where the error due to the angular distribution of the emitted photons is indicated with (model). This last uncertainty is conservatively calculated as the difference between the S factors obtained without any assumption on the angular distribution and assuming the Mukhamedzhanov angular distribution. These results are consistent with Eqs. (4) and (5) within errors.

Finally, the analysis has been performed using wider and wider portions of the spectra, up to $500 < E_\gamma < 2500$ keV considering the whole spectra or only regions of them, to exclude possible local bias inside the energy interval considered in this Letter. All the obtained results are fully consistent with those presented here.

The present results provide the first direct measurement of the $^2\mathrm{H}(\alpha,\gamma)^6\mathrm{Li}$ cross section inside the BBN energy range. They are in good agreement with the theoretical values of Mukhamedzhanov [24] and about 20% lower than the theoretical predictions of Hammache [15]. Figure 3 shows the presently obtained astrophysical S factor compared with literature data and theoretical curves.

The reaction rate calculated from our new S factor values by rescaling the $E1$ component of the Mukhamedzhanov theoretical curve so that $E1 + E2$ match our data, is significantly lower than the widely adopted Caughlan and Fowler (CF88) [25] rate. Our new rate has then been used to compute the amount of ^{6}Li produced in BBN, with the widely adopted Smith, Kawano, and Malaney (SKM) code [26]. A value of 880.1 s has been used for the neutron lifetime, and 6.047×10^{-10} for the final baryon-to-photon ratio [4]. The resulting abundance is $^6\mathrm{Li}/H = (0.74 \pm 0.16) \times 10^{-14}$, 34% lower than the value obtained when using CF88. In order to compute the $^6\mathrm{Li}/^7\mathrm{Li}$ isotopic ratio from BBN, up to date information on ^{7}Li production is also needed. A recent reevaluation of the $^3\mathrm{H}(\alpha,\gamma)^7\mathrm{Be}$ reaction rate [27] uses an excitation function that is consistent within 2% with the only recent experimental data on this reaction [5,6] at energies below 0.3 MeV, most relevant for BBN. Using this rate [27], $^7\mathrm{Li}/H = (5.1 \pm 0.4) \times 10^{-10}$ is found, 15% higher than when using CF88. The resulting lithium isotopic ratio is $^6\mathrm{Li}/^7\mathrm{Li} = (1.5 \pm 0.3) \times 10^{-5}$. The error for $^6\mathrm{Li}/^7\mathrm{Li}$ is mainly due to the 22% uncertainty on ^{6}Li, because the ^{7}Li abundance is known at the 8% level [28]. The calculations have then been repeated using the PARTHENOPE (Naples) code [29] instead of SKM, with consistent results. The $^6\mathrm{Li}/^7\mathrm{Li}$ isotopic abundance ratio inferred from our experimental results is lower than the previous values of $2^{+3}_{-2} \times 10^{-5}$ [11] and 2.3×10^{-5} [30]. Also, it is much lower than the one obtained from the reported ^{6}Li detections in metal-poor stars and in the Small Magellanic Cloud [31].

In summary, the cross section of the $^2\mathrm{H}(\alpha,\gamma)^6\mathrm{Li}$ nuclear reaction controlling BBN production of ^{6}Li has been measured, providing the first data points at BBN energies. Using the new $^2\mathrm{H}(\alpha,\gamma)^6\mathrm{Li}$ cross section and the previous LUNA data on BBN production of ^{7}Li, a BBN lithium abundance ratio of $^6\mathrm{Li}/^7\mathrm{Li} = (1.5 \pm 0.3) \times 10^{-5}$ is obtained, firmly ruling out standard BBN production as a possible explanation for the reported ^{6}Li detections. Pregalactic ^{6}Li production mechanisms have also been previously ruled out [32]. As a result, possible remaining scenarios explaining a global $^6\mathrm{Li}/^7\mathrm{Li}$ level of a few percent as reported [7,8,10,33,34] may be, under very special conditions, a stellar flare *in situ* production of ^{6}Li [32] or nonstandard physics solutions [35–38]. Cosmic ^{6}Li is clearly a highly interesting probe of physics beyond the standard model.

The authors are indebted to F. L. Villante (INFN-LNGS) for informative conversations on BBN calculations, and to the mechanical and electronic workshops of LNGS for technical support. Financial support by INFN, FAI, DFG (Grant No. BE 4100-2/1), NAVI (Grant No. HGF VH-VI-417), and OTKA (Grant No. K101328) is gratefully acknowledged.

*Deceased.
†Present address: Landesamt für Umwelt, Gesundheit und Verbraucherschutz Brandenburg, Potsdam, Germany.
‡Present address: CPPM, Université d'Aix-Marseille, CNRS/IN2P3, Marseille, France.

[§]Present address: PTB, Braunschweig, Germany.
[‖]Corresponding author:carlo.gustavino@roma1.infn.it
[¶]Present address: GSI, Darmstadt, Germany.
[**]Present address: University of Warsaw, Warsaw, Poland.

[1] B. D. Fields, Annu. Rev. Nucl. Part. Sci. **61**, 47 (2011).
[2] M. Spite and F. Spite, Nature (London) **297**, 483 (1982).
[3] G. Hinshaw *et al.*, Astrophys. J. Suppl. Ser. **208**, 19 (2013).
[4] P. A. R. Ade *et al.* (Planck Collaboration), arXiv: 1303.5076v1 [Astron. Astrophys. (to be published)].
[5] D. Bemmerer *et al.*, Phys. Rev. Lett. **97**, 122502 (2006).
[6] F. Confortola *et al.*, Phys. Rev. C **75**, 065803 (2007).
[7] M. Asplund, D. L. Lambert, P. E. Nissen, F. Primas, and V. V. Smith, Astrophys. J. **644**, 229 (2006).
[8] M. Asplund and J. Meléndez, AIP Conf. Proc. **990**, 342 (2008).
[9] K. Lind, J. Melendez, M. Asplund, R. Collet, and Z. Magic, Astron. Astrophys. **554**, A96 (2013).
[10] M. Steffen, R. Cayrel, E. Caffau, P. Bonifacio, H.-G. Ludwig, and M. Spite, Mem. Soc. Astron. Ital. **22**, 152 (2012).
[11] P. D. Serpico, S. Esposito, F. Iocco, G. Mangano, G. Miele, and O. Pisanti, J. Cosmol. Astropart. Phys. 12 (2004) 010.
[12] R. G. H. Robertson, P. Dyer, R. Warner, R. Melin, T. Bowles, A. McDonald, G. Ball, W. Davies, and E. Earle, Phys. Rev. Lett. **47**, 1867 (1981).
[13] P. Mohr, V. Kölle, S. Wilmes, U. Atzrott, G. Staudt, J. Hammer, H. Krauss, and H. Oberhummer, Phys. Rev. C **50**, 1543 (1994).
[14] J. Kiener, H. Gils, H. Rebel, S. Zagromski, G. Gsottschneider, N. Heide, H. Jelitto, J. Wentz, and G. Baur, Phys. Rev. C **44**, 2195 (1991).
[15] F. Hammache *et al.*, Phys. Rev. C **82**, 065803 (2010).
[16] F. E. Cecil, J. Yan, and C. S. Galovich, Phys. Rev. C **53**, 1967 (1996).
[17] A. Caciolli *et al.*, Eur. Phys. J. A **39**, 179 (2009).
[18] H. Costantini, A. Formicola, G. Imbriani, M. Junker, C. Rolfs, and F. Strieder, Rep. Prog. Phys. **72**, 086301 (2009).
[19] C. Broggini, D. Bemmerer, A. Guglielmetti, and R. Menegazzo, Annu. Rev. Nucl. Part. Sci. **60**, 53 (2010).
[20] A. Formicola *et al.*, Nucl. Instrum. Methods Phys. Res., Sect. A **507**, 609 (2003).
[21] M. Anders *et al.*, Eur. Phys. J. A **49**, 28 (2013).
[22] M. Erhard *et al.*, in Annual Report 2004, Institute of Nuclear and Hadron Physics, FZR-423, 2005, edited by W. Enghardt *et al.* (unpublished).
[23] M. Anders, Ph.D. thesis, Technische Universität Dresden, 2013.
[24] A. M. Mukhamedzhanov, L. D. Blokhintsev, and B. F. Irgaziev, Phys. Rev. C **83**, 055805 (2011).
[25] G. Caughlan and W. Fowler, At. Data Nucl. Data Tables **40**, 283 (1988).
[26] M. S. Smith, L. H. Kawano, and R. A. Malaney, Astrophys. J. Suppl. Ser. **85**, 219 (1993).
[27] A. Kontos, E. Uberseder, R. deBoer, J. Görres, C. Akers, A. Best, M. Couder, and M. Wiescher, Phys. Rev. C **87**, 065804 (2013).
[28] A. Coc, J. Uzan, and E. Vangioni, arXiv:1403.6694.
[29] O. Pisanti, A. Cirillo, S. Esposito, F. Iocco, G. Mangano, G. Miele, and P. D. Serpico, Comput. Phys. Commun. **178**, 956 (2008).
[30] A. Coc, S. Goriely, Y. Xu, M. Saimpert, and E. Vangioni, Astrophys. J. **744**, 158 (2012).
[31] J. C. Howk, N. Lehner, B. D. Fields, and G. J. Mathews, Nature (London) **489**, 121 (2012).
[32] N. Prantzos, Astron. Astrophys. **542**, A67 (2012).
[33] V. V. Smith, D. L. Lambert, and P. E. Nissen, Astrophys. J. **408**, 262 (1993).
[34] R. Cayrel, M. Spite, F. Spite, E. Vangioni-Flam, M. Cassé, and J. Audouze, Astron. Astrophys. **343**, 923 (1999).
[35] K. Jedamzik and M. Pospelov, New J. Phys. **11**, 105028 (2009).
[36] H. Djapo, I. Boztosun, G. Kocak, and A. B. Balantekin, Phys. Rev. C **85**, 044602 (2012).
[37] M. Pospelov and J. Pradler, Annu. Rev. Nucl. Part. Sci. **60**, 539 (2010).
[38] M. Kusakabe, T. Kajino, R. N. Boyd, T. Yoshida, and G. J. Mathews, Phys. Rev. D **76**, 121302 (2007).